Probing Hadronization and Quark-Gluon Plasma Using Collinear-Drop Jet Observables

Oleh Fedkevych

Physics and Astronomy Department, Georgia State University, Atlanta, GA
Center for Frontiers in Nuclear Science, Stony Brook University, Stony Brook, NY
Jefferson Lab, Newport News, VA

May 22, 2025

In collaboration with Yang-Ting Chien

(Almost) classical picture: accelerated charges radiate

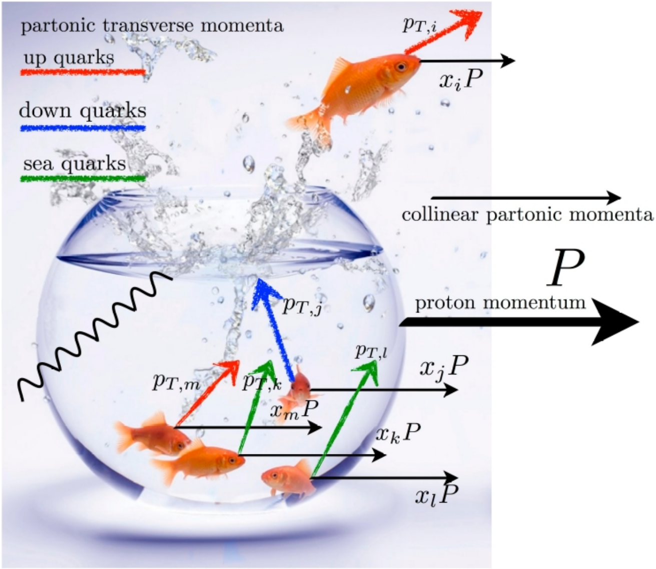

Credit: http://www.quantumdiaries.org/tag/physics/

(Almost) classical picture: accelerated charges radiate

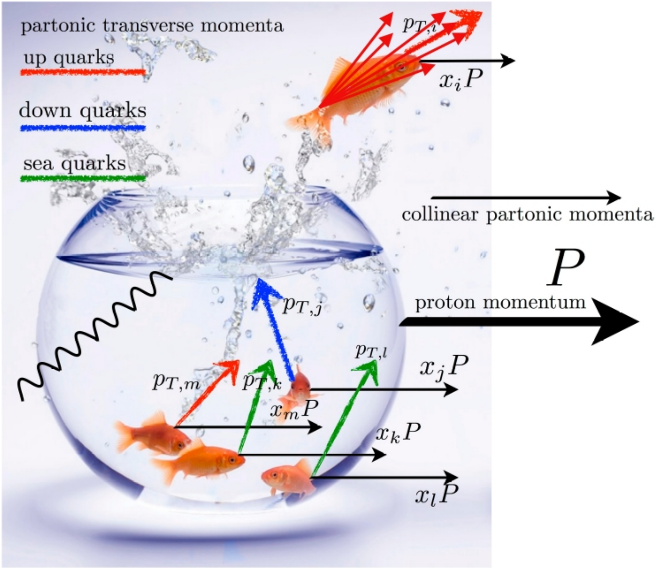

Credit: http://www.quantumdiaries.org/tag/physics/

(Almost) classical picture: accelerated charges radiate

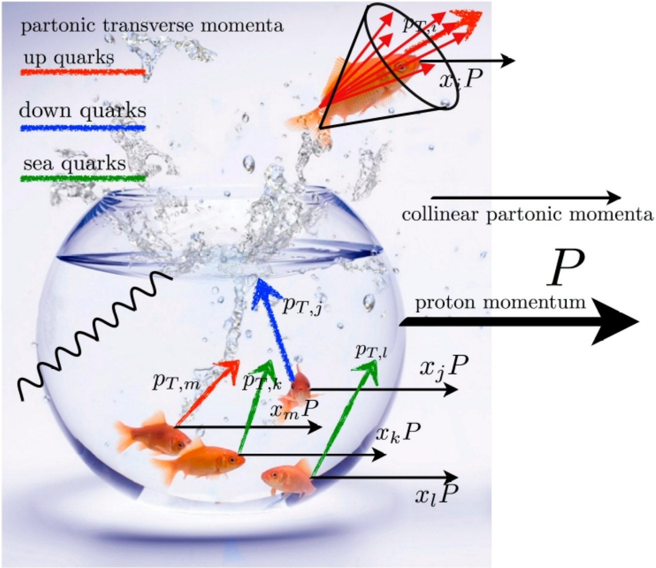

Credit: http://www.quantumdiaries.org/tag/physics/

(Almost) classical picture: accelerated charges radiate

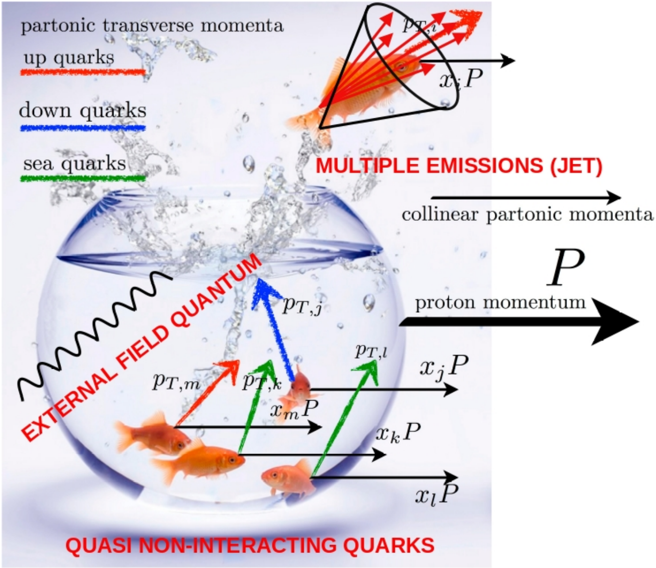

Credit: http://www.quantumdiaries.org/tag/physics/

In 1977 Sterman and Weinberg proposed their jet reconstruction algorithm

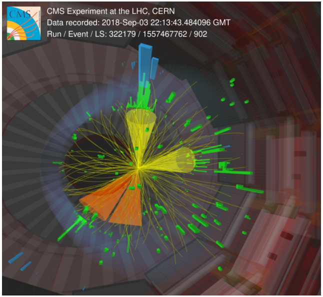

To study jets, we consider the partial cross section $\sigma(E, \theta, \Omega, \epsilon, \delta)$ for e^+e^- hadron production events, in which all but a fraction $\epsilon \ll 1$ of the total e^+e^- energy E is emitted within some pair of oppositely directed cones of half-angle $\delta \ll 1$, lying within two fixed cones of solid angle Ω (with $\pi\delta^2 \ll \Omega \ll 1$) at an angle θ to the e^+e^- beam line. We expect this to be measurable for $m=0$, because the only quarks or gluons which are likely to be diffracted or radiated away from a calorimeter at θ have very long wavelength, and so carry negligible energy. Thus σ should be free of mass singularities for $m \to 0$, and calculable

Left: jet production process (CMS). Right: jet definition from the work of Sterman and Weinberg PhysRevLett.39.1436

Looking inside jets: jet substructure observables

- In principle, any function which takes all particles inside jet can be seen as a jet substructure observable. For example, jet multiplicity (number of jet constituents)
- However, to apply perturbation theory, we require observables to satisfy the infrared-collinear (IRC) safety requirement.

An example of the IRC-safe observable is given by the jet angularities:

$$\lambda_\alpha = \sum_{i \in \text{jet}} \frac{p_{t,i}}{p_{t,\text{jet}}} \left(\frac{\Delta R_{ij}}{R} \right)^\alpha , \quad \alpha > 0$$

A particular case $\alpha = 2$ yields a jet mass

$$m_{\text{jet}}^2 = \left(\sum_{i \in \text{jet}} p_i \right)^2 , \quad or \quad \rho = \frac{m_{\text{jet}}^2}{p_t^2 R^2} \sim \lambda_2$$

Jet angularity was originally introduced in hep-ph/0303051 and its generalized version in 1408.3122

Soft and Collinear limit of QCD

A probability of a single emission can be expressed in terms of

$$z = \frac{E_g}{E_q + E_g}, \quad 1 - \cos\theta = \frac{m^2}{2E_q\, E_g}$$

and in the soft and collinear limit of QCD one get a standard di-log expression

$$P(z, \theta^2)\, dz\, d\theta^2 \sim \alpha_S\, d\left(\log\frac{1}{z}\right)\, d\left(\log\frac{1}{\theta^2}\right)$$

which allows to factorize matrix elements for n-emissions

$$\mathcal{M}_{2\to n} \approx \mathcal{M}_{2\to n-1}\, P(z, \theta^2)\, dz\, d\theta^2$$

and so on.

Lund Plane landscape

If we assume that all emissions are uncorrelated and distributed according to $P(z,\theta^2)\, dz\, d\theta^2 \sim \alpha_S d\left(\log\frac{1}{z}\right)\, d\left(\log\frac{1}{\theta^2}\right)$ then we can introduce the jet emission plane (Lund Plane)

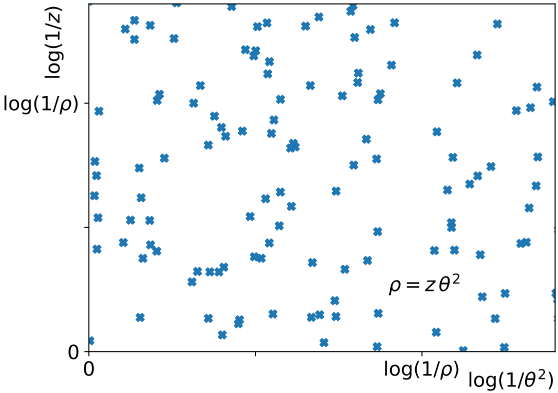

Emissions are uniformly distributed in the Lund Plane $P(z,\theta^2) \sim \alpha_S$

Lund Plane landscape

If we assume that all emissions are uncorrelated and distributed according to $P(z, \theta^2)\, dz\, d\theta^2 \sim \alpha_S d\left(\log \frac{1}{z}\right)\, d\left(\log \frac{1}{\theta^2}\right)$ then we can introduce the jet emission plane (Lund Plane)

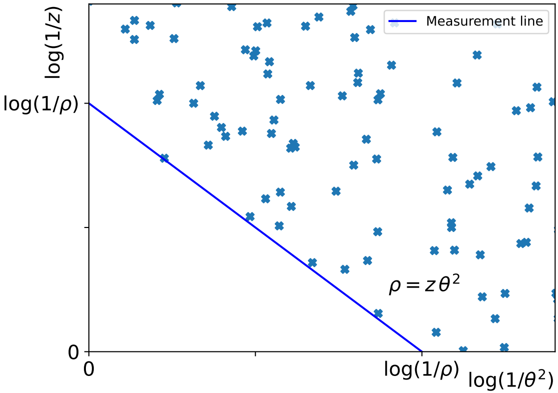

IRC-safe observables set finite no-emission areas

It is convenient to consider cumulative distribution $\Sigma(x \le \rho)$

$$\Sigma(\text{emit in } i) = \alpha_S \frac{1}{2} \frac{\log^2 \rho}{N}$$

$$\Sigma(\text{no emission in } i) = 1 - P(\text{emit in } i)$$

$$\Sigma(x \le \rho) = \lim_{N\to\infty} (1 - P(\text{emit in } i))^N$$

$$\Sigma(x \le \rho) = \lim_{N\to\infty} \left(1 - \alpha_S \frac{1}{2} \frac{\log^2 \rho}{N}\right)^N$$

$$\Sigma(x \le \rho) = \exp\left(-\alpha_S \frac{1}{2} \log^2 \rho\right)$$

$$p(\rho) = \frac{d}{d\rho} \exp\left(-\alpha_S \frac{1}{2} \log^2 \rho\right)$$

Note that our result is finite if $\rho \to 0$!

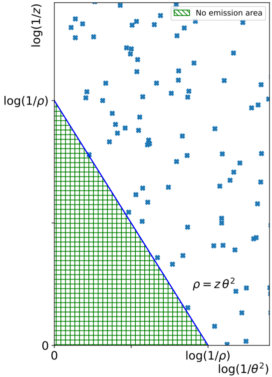

We divide no-emission area into N pixels.

For more details see lectures of A. Larkoski arXiv:1709.06195

A realistic calculation

- Emissions are correlated and α_S is scale dependent

$$\frac{\alpha_S}{2\pi} \to \frac{1}{2\pi}\frac{\alpha_S}{1-\xi} - \frac{\alpha_S^2}{2\pi}\frac{\beta_1}{\beta_0}\frac{\log(1-\xi)}{(1-\xi)^2} + \frac{K}{(2\pi)^2}\frac{\alpha_S^2}{(1-\xi)^2},$$

where $\xi = \alpha_S(\mu_0^2)\beta_0 \log(\mu_0^2/\mu^2)$.

- The answer (usually) has a general structure

$$\begin{aligned} \Sigma(x \le \rho) &= \int d\mathcal{B}\frac{d\sigma_\delta}{d\mathcal{B}}\frac{\exp(-\gamma_E \mathcal{R}')}{\Gamma(1+R')}\exp\left(-\mathcal{R}\right), \\ L &= \log(1/\rho), \quad \mathcal{R}' = \partial\mathcal{R}/\partial L \end{aligned}$$

where

$$\mathcal{R} = L g_1(\alpha_S L) + g_2(\alpha_S L) + \alpha_S g_3(\alpha_S L) + \dots$$

is a Sudakov no-emission probability (“radiator”).

The original calculation by Dasgupta et al in arXiv:1207.1640

$$
\begin{aligned}
\mathcal{R}^{\mathrm{NLL}} &= \frac{C_{F/A}}{2\pi}\frac{1}{\alpha_S\beta_0^2}\left[W(1-\lambda_\rho) - 2W\left(1-\frac{\lambda_\rho}{2}\right)\right] \\
&- \frac{C_{F/A}}{2\pi}\frac{\beta_1}{\beta_0^3}\left[V(1-\lambda_\rho) - 2\,V\left(1-\frac{\lambda_\rho}{2}\right)\right] \\
&- \frac{C_{F/A}}{2\pi}\frac{K}{2\pi\beta_0^2}\left(\log(1-\lambda_\rho) - 2\log\left(1-\frac{\lambda_\rho}{2}\right)\right) - \frac{C_{F/A}}{\pi\beta_0}B_q\,\log\left(1-\frac{\lambda_\rho}{2}\right),
\end{aligned}
$$

where $W(x) = x\log(x)$, $V(x) = \frac{1}{2}\log(x)^2 + \log(x)$, $\lambda_\rho = 2\alpha_s\beta_0\log(1/\rho)$.

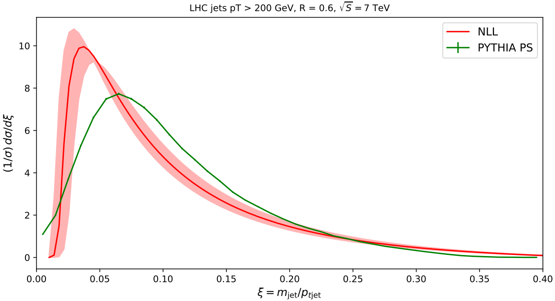

...but QCD is very complicated!

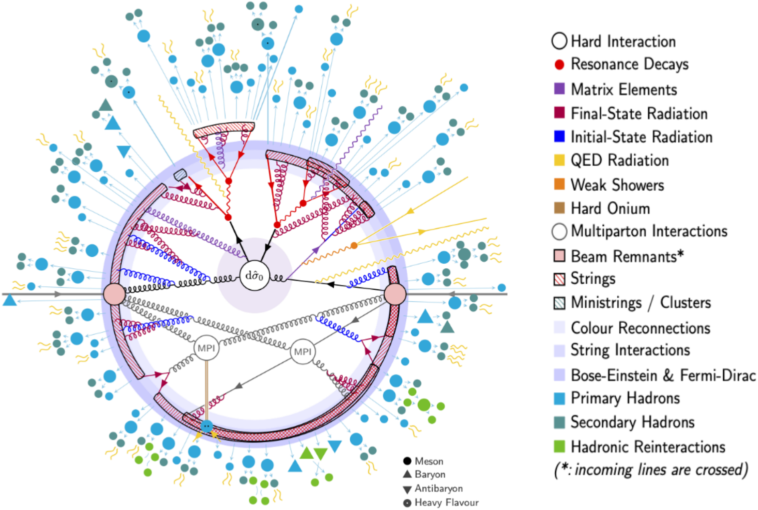

Image credit: Peter Skands.

...but QCD is very complicated!

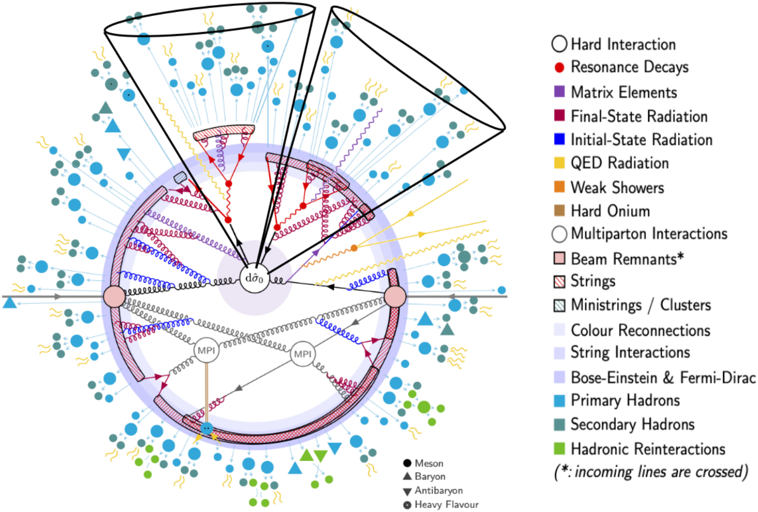

Image credit: Peter Skands.

...but QCD is very complicated!

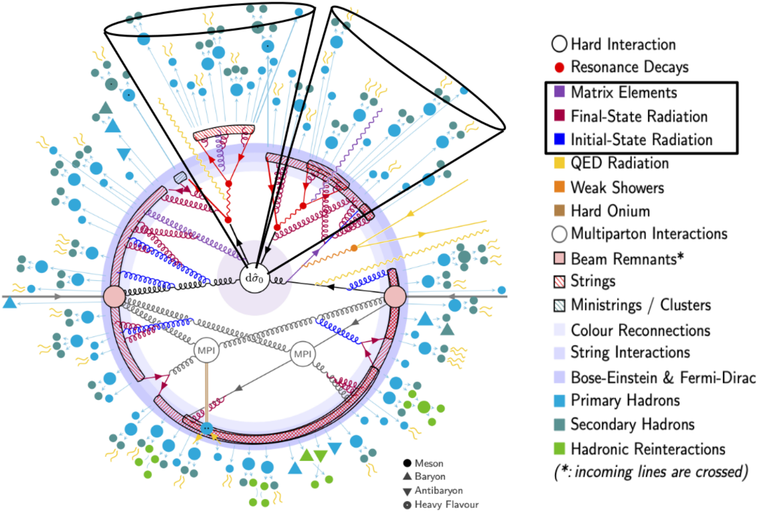

Image credit: Peter Skands.

...but QCD is very complicated!

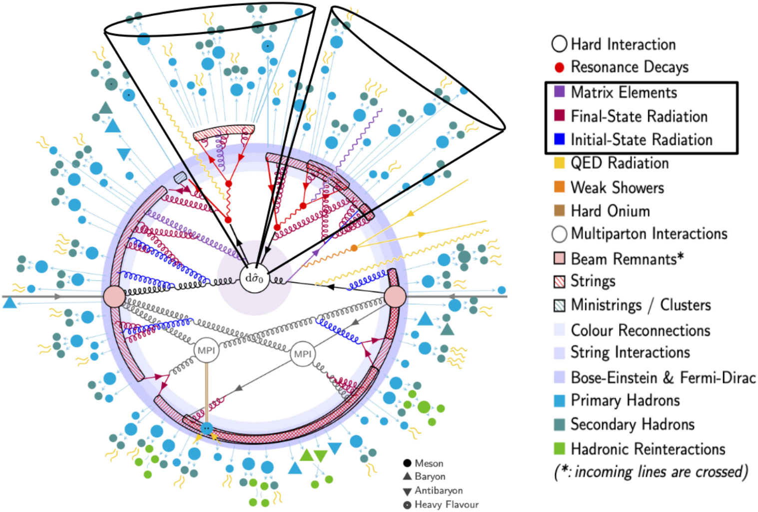

Image credit: Peter Skands.

Soft radiation from MPI (UE) contaminates jets

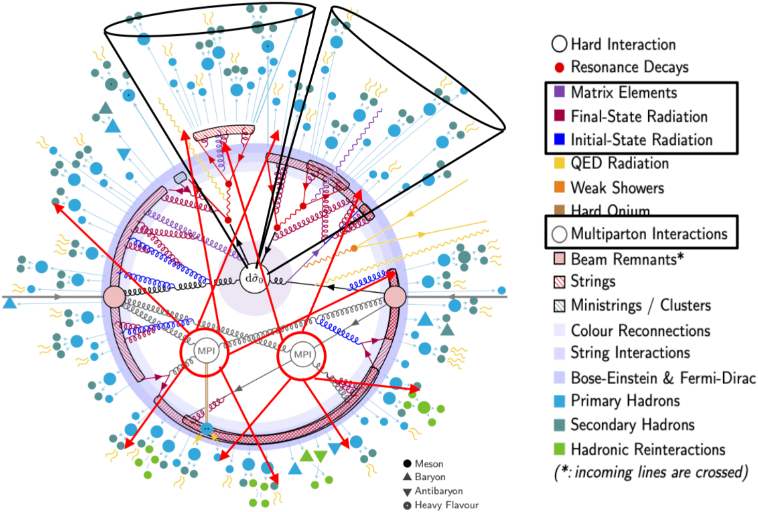

Image credit: Peter Skands.

SoftDrop grooming condition: $\frac{\min(p_{ti}, p_{tj})}{p_{ti}+p_{tj}} > z_{\rm cut} \left(\frac{\Delta R_{ij}}{R}\right)^{\beta}$

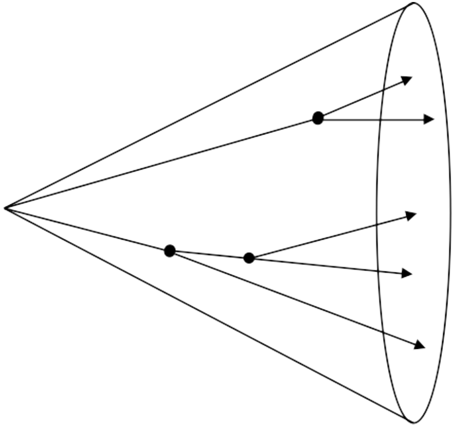

- Set values of $z_{\rm cut}$ and β
- Recluster jet into two branches
- Check the SoftDrop condition
- If "True" stop the procedure
- Otherwise reject softest branch and repeat
- This procedure is IRC-safe

SoftDrop grooming condition: $\frac{\min(p_{ti}, p_{tj})}{p_{ti}+p_{tj}} > z_{\rm cut} \left(\frac{\Delta R_{ij}}{R}\right)^\beta$

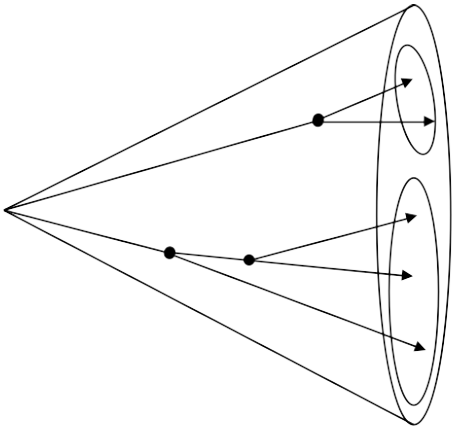

- Set values of $z_{\rm cut}$ and β
- Recluster jet into two branches
- Check the SoftDrop condition
- If "True" stop the procedure
- Otherwise reject softest branch and repeat
- This procedure is IRC-safe

SoftDrop grooming condition: $\frac{\min(p_{ti}, p_{tj})}{p_{ti}+p_{tj}} > z_{\mathrm{cut}} \left(\frac{\Delta R_{ij}}{R}\right)^{\beta}$

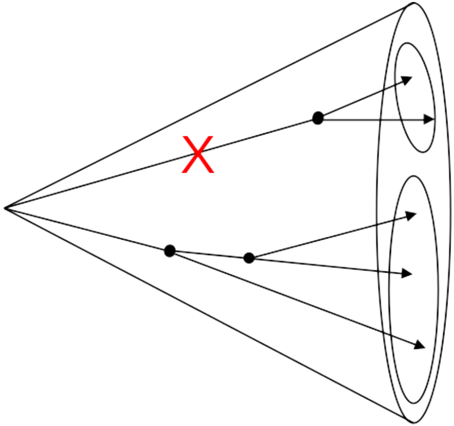

- Set values of z_{cut} and β
- Recluster jet into two branches
- Check the SoftDrop condition
- If "True" stop the procedure
- Otherwise reject softest branch and repeat
- This procedure is IRC-safe

SoftDrop grooming condition: $\frac{\min(p_{ti}, p_{tj})}{p_{ti}+p_{tj}} > z_{\rm cut}\left(\frac{\Delta R_{ij}}{R}\right)^{\beta}$

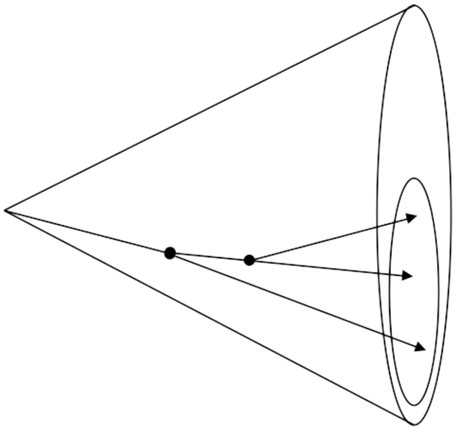

- Set values of $z_{\rm cut}$ and β
- Recluster jet into two branches
- Check the SoftDrop condition
- If "True" stop the procedure
- Otherwise reject softest branch and repeat
- This procedure is IRC-safe

SoftDrop grooming condition: $\frac{\min(p_{ti}, p_{tj})}{p_{ti}+p_{tj}} > z_{\text{cut}} \left(\frac{\Delta R_{ij}}{R}\right)^{\beta}$

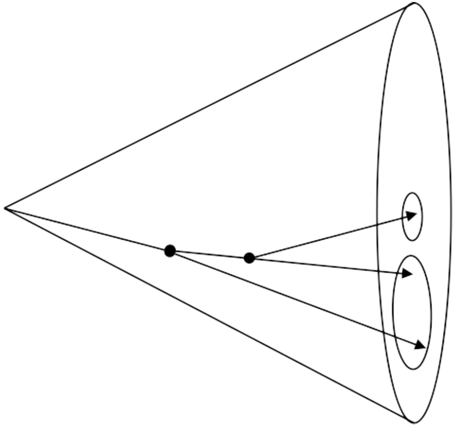

- Set values of z_{cut} and β
- Recluster jet into two branches
- Check the SoftDrop condition
- If "True" stop the procedure
- Otherwise reject softest branch and repeat
- This procedure is IRC-safe

SoftDrop grooming condition: $\frac{\min(p_{ti}, p_{tj})}{p_{ti}+p_{tj}} > z_{\text{cut}} \left(\frac{\Delta R_{ij}}{R}\right)^{\beta}$

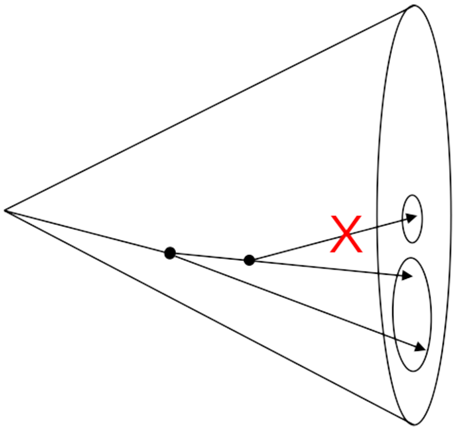

- Set values of z_{cut} and β
- Recluster jet into two branches
- Check the SoftDrop condition
- If "True" stop the procedure
- Otherwise reject softest branch and repeat
- This procedure is IRC-safe

SoftDrop grooming condition: $\frac{\min(p_{ti}, p_{tj})}{p_{ti}+p_{tj}} > z_{\text{cut}} \left(\frac{\Delta R_{ij}}{R}\right)^{\beta}$

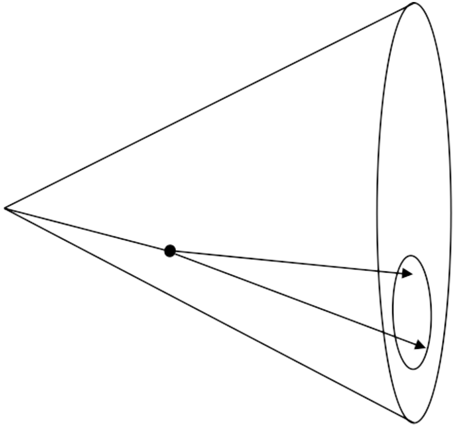

- Set values of z_{cut} and β
- Recluster jet into two branches
- Check the SoftDrop condition
- If "True" stop the procedure
- Otherwise reject softest branch and repeat
- This procedure is IRC-safe

SoftDrop grooming condition: $\frac{\min(p_{ti}, p_{tj})}{p_{ti}+p_{tj}} > z_{\mathrm{cut}} \left(\frac{\Delta R_{ij}}{R}\right)^{\beta}$

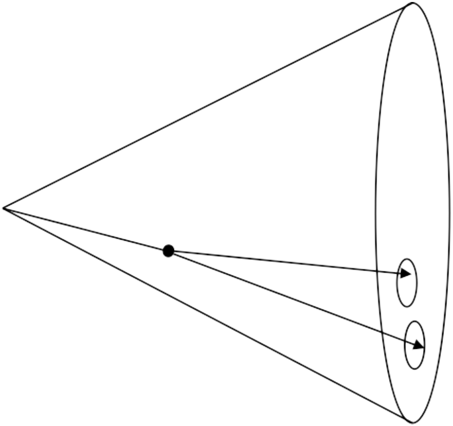

- Set values of z_{cut} and β
- Recluster jet into two branches
- Check the SoftDrop condition
- If "True" stop the procedure
- Otherwise reject softest branch and repeat
- This procedure is IRC-safe

SoftDrop grooming condition: $\frac{\min(p_{ti}, p_{tj})}{p_{ti}+p_{tj}} > z_{\mathrm{cut}} \left(\frac{\Delta R_{ij}}{R}\right)^{\beta}$

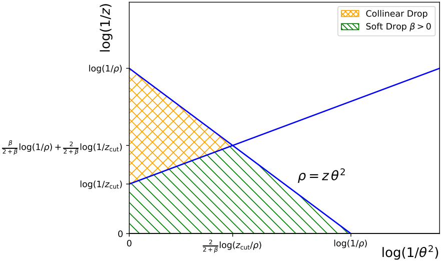

- Set values of z_{cut} and β
- Recluster jet into two branches
- Check the SoftDrop condition
- If "True" stop the procedure
- Otherwise reject softest branch and repeat
- This procedure is IRC-safe

SoftDrop results by Marzani et al in arXiv:1712.05105

$$
\begin{aligned}
R_{\rm SD}^{\rm NLL} \;=\;& \frac{C_F}{2\pi}\frac{1}{\alpha_S\beta_0^2}\left[\frac{2+\beta}{1+\beta}W\left(1-\frac{\lambda_z+(1+\beta)\lambda_\rho}{2+\beta}\right)-2W\left(1-\frac{\lambda_\rho}{2}\right)-\frac{1}{1+\beta}W\left(1-\lambda_z\right)\right]\\
+\;& \frac{C_F}{2\pi}\frac{\beta_1}{\beta_0^3}\left[\frac{2+\beta}{1+\beta}V\left(1-\frac{\lambda_z+(1+\beta)\lambda_\rho}{2+\beta}\right)-\frac{1}{1+\beta}V(1-\lambda_z)-2\,V\left(1-\frac{\lambda_\rho}{2}\right)\right]\\
-\;& \frac{C_F}{2\pi}\frac{K}{2\pi\beta_0^2}\left(\frac{2+\beta}{1+\beta}\log\left(1-\frac{\lambda_z+(1+\beta)\lambda_\rho}{2+\beta}\right)-\frac{1}{1+\beta}\log\left(1-\lambda_z\right)-2\log\left(1-\frac{\lambda_\rho}{2}\right)\right)\\
-\;& \frac{C_F}{\pi\beta_0}B_q\,\log\left(1-\frac{\lambda_\rho}{2}\right),
\end{aligned}
$$

where $W(x) = x\log(x)$, $V(x) = \frac{1}{2}\log(x)^2 + \log(x)$, $\lambda_\rho = 2\alpha_s\beta_0\log(1/\rho)$.

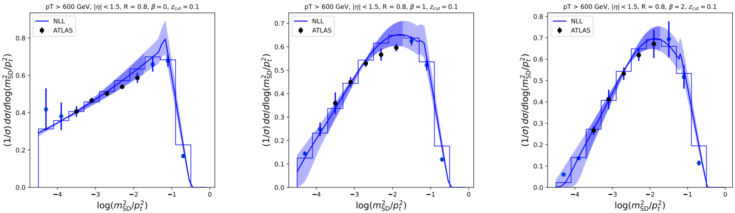

ATLAS measurements 1711.08341

CollinearDrop condition is opposite to SoftDrop

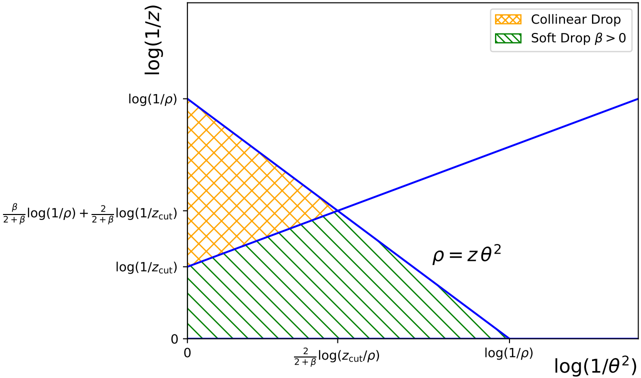

CollinearDrop condition is opposite to the SoftDrop condition $\frac{\min(p_{ti}, p_{tj})}{p_{ti}+p_{tj}} > z_{\rm cut}\left(\frac{\Delta R_{ij}}{R}\right)^{\beta}$ which allows to pick up soft and soft-wide angle emissions.

See "Resummation of Flattened Jet Angularity Using Soft-Collinear Effective Theory" by Yang-Ting Chien and arXiv:1907.11107

CollinearDrop condition is opposite to SoftDrop

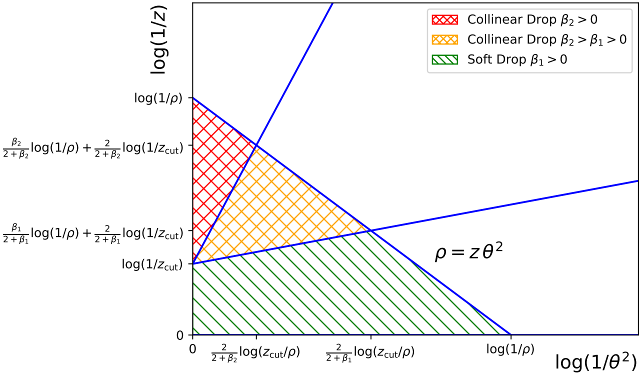

CollinearDrop condition is opposite to the SoftDrop condition $\frac{\min(p_{ti}, p_{tj})}{p_{ti}+p_{tj}} > z_{\mathrm{cut}} \left(\frac{\Delta R_{ij}}{R}\right)^{\beta}$ which allows to pick up soft and soft-wide angle emissions.

See "Resummation of Flattened Jet Angularity Using Soft-Collinear Effective Theory" by Yang-Ting Chien and arXiv:1907.11107

Main result for Collinear Drop is given by

$$
\begin{aligned}
R_{\mathrm{CD}}^{\beta_2,\beta_1} &= \frac{C_F}{2\pi}\,\frac{1}{\alpha_S\,\beta_0^2}\left[\frac{2+\beta_2}{1+\beta_2}\,W\!\left(1-\frac{\lambda_z+(1+\beta_2)\lambda_\rho}{2+\beta_2}\right)-\frac{2+\beta_1}{1+\beta_1}\,W\!\left(1-\frac{\lambda_z+(1+\beta_1)\lambda_\rho}{2+\beta_1}\right)\right.\\
&+ \left.\frac{\beta_2-\beta_1}{(1+\beta_2)(1+\beta_1)}W(1-\lambda_z)\right]\\
&+ \frac{C_F}{2\pi}\,\frac{\beta_1}{\beta_0^3}\left[\frac{2+\beta_2}{1+\beta_1}V\!\left(1-\frac{\lambda_z+(1+\beta_2)\lambda_\rho}{2+\beta_2}\right)-\frac{2+\beta_2}{1+\beta_1}V\!\left(1-\frac{\lambda_z+(1+\beta_2)\lambda_\rho}{2+\beta_2}\right)\right.\\
&+ \left.\frac{\beta_2-\beta_1}{(1+\beta_2)(1+\beta_1)}\,V\,(1-\lambda_z)\right]\\
&+ \frac{C_F}{2\pi}\,\frac{K}{2\pi\beta_0^2}\left[\frac{2+\beta_2}{1+\beta_2}\,\log\!\left(1-\frac{\lambda_z+(1+\beta_2)\lambda_\rho}{2+\beta_2}\right)-\frac{2+\beta_1}{1+\beta_1}\,\log\!\left(1-\frac{\lambda_z+(1+\beta_1)\lambda_\rho}{2+\beta_1}\right)\right.\\
&- \left.\frac{\beta_2-\beta_1}{(1+\beta_1)(1+\beta_2)}\log(1-\lambda_z)\right],
\end{aligned}
$$

where $W(x) = x\log(x)$, $V(x) = \frac{1}{2}\log(x)^2 + \log(x)$, $\lambda_\rho = 2\alpha_s\beta_0\log(1/\rho)$ and $\lambda_z = 2\alpha_s\beta_0\log(1/z_{\mathrm{cut}})$

CollinearDrop: LHC setup

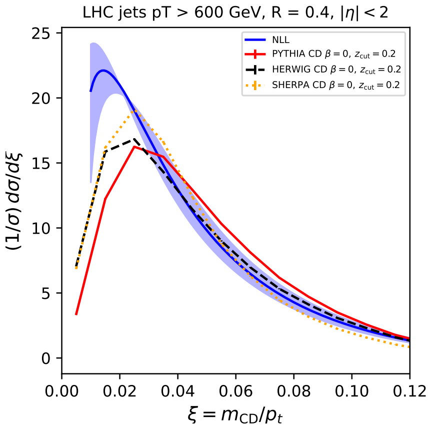

- We consider ATLAS setup: $\sqrt{S} = 13$ TeV, $p_t > 600$, $|\eta| < 2$
- Pythia, Herwig and Sherpa MC simulations are at the parton level without UE
- Differences at small values of ξ are due to the Landau pole treatment.

CollinearDrop: RHIC setup

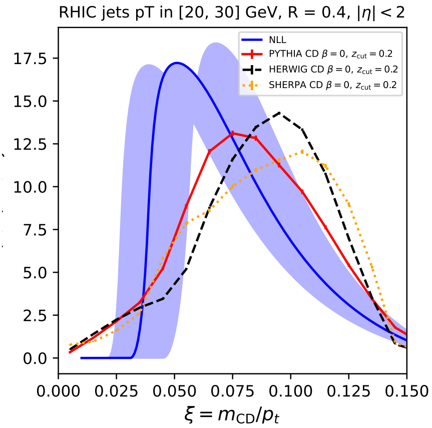

- We consider STAR setup: $\sqrt{S} = 0.2$ TeV, $p_t \in [20, 30]$, $|\eta| < 0.6$
- Pythia, Herwig and Sherpa MC simulations are at the parton level without UE
- Differences at small values of ξ are due to the Landau pole treatment.

Soft radiation from MPI (UE) contaminates jets

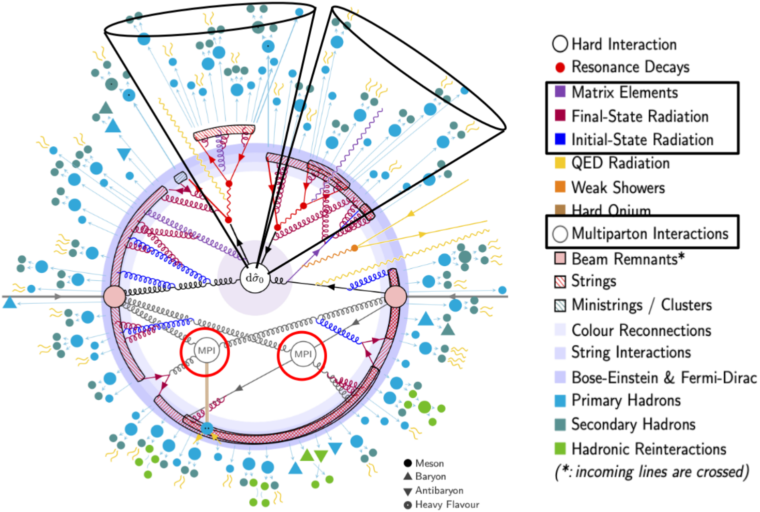

Image credit: Peter Skands.

Soft radiation from MPI (UE) contaminates jets

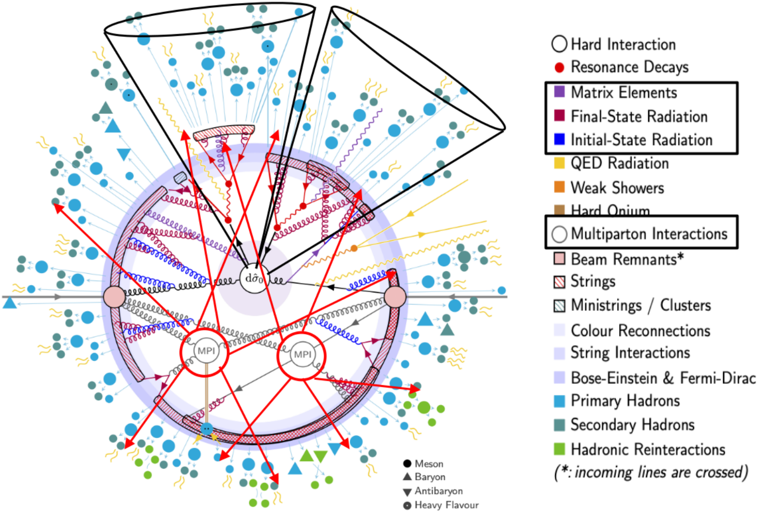

Image credit: Peter Skands.

Hadronization partons and turns them into hadrons

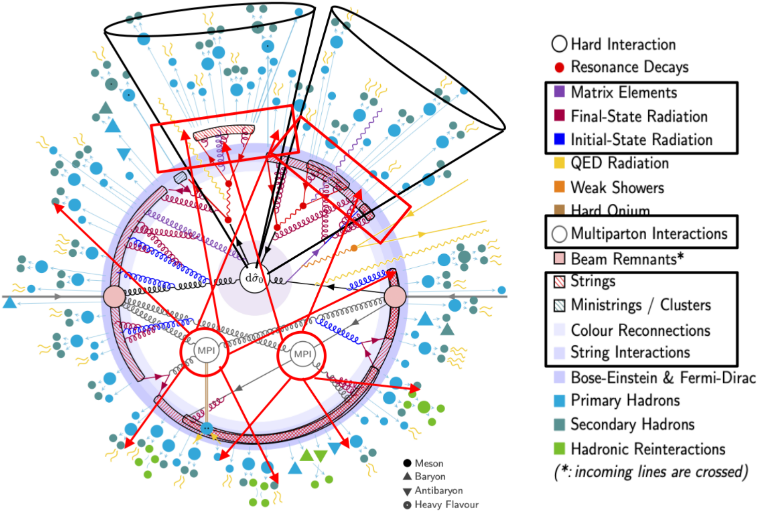

Image credit: Peter Skands.

Unstable hadrons decay and change jet substructure

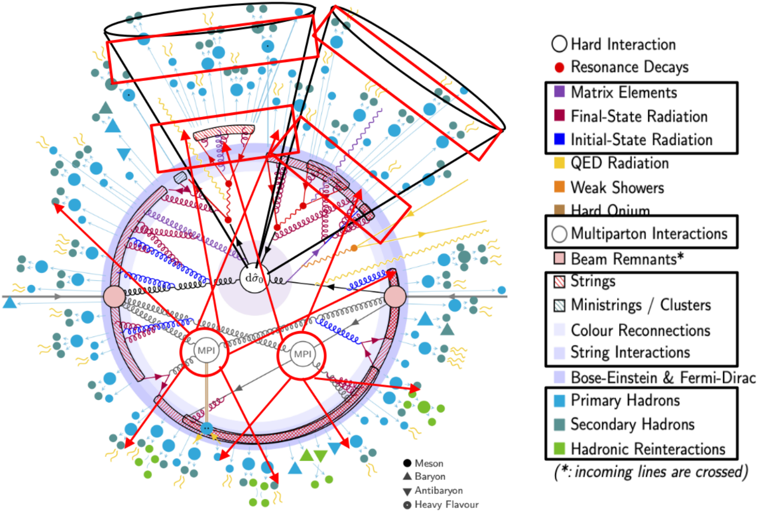

Image credit: Peter Skands.

Parton to hadron level transition; credit G. Soyez

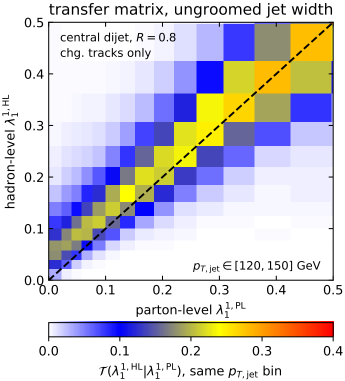

- Transfer matrix can be extracted from MC
- One needs to "put event generation on pause" when parton shower reach non-perturbative scale and calculate $\lambda_\alpha^{\mathrm{PL}}$
- After that one "resume" event generation and calculate $\lambda_\alpha^{\mathrm{HL}}$
- The correlations between $\lambda_\alpha^{\mathrm{PL}}$ and $\lambda_\alpha^{\mathrm{HL}}$ are used to build TMs

The transfer matrices were introduced by Reichetl et al in arXiv:2112.09545

ATLAS: impact of non-perturbative corrections

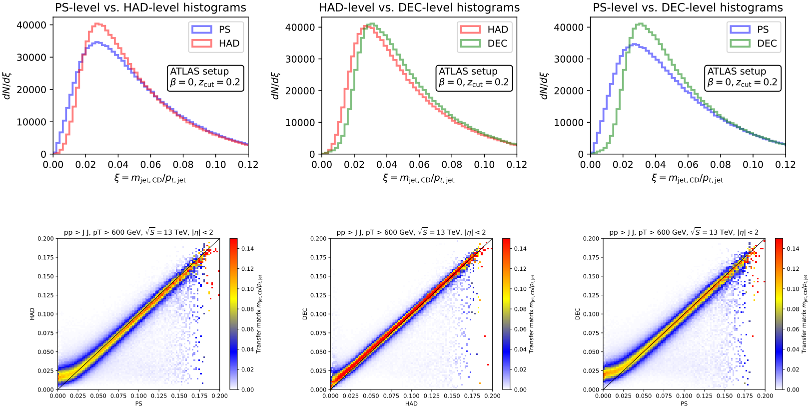

Non-perturbative corrections usually shift distributions towards larger observable values. Here we consider parton-to-hadron transition and hadronic decays separately.

ATLAS: impact of non-perturbative corrections

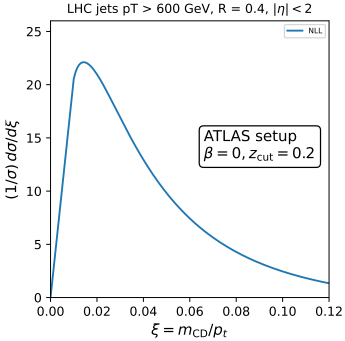

- Transfer matrix can be extracted from MC
- One needs to "put event generation on pause" when parton shower reach non-perturbative scale and calculate $\lambda_\alpha^{\mathrm{PL}}$
- After that one "resume" event generation and calculate $\lambda_\alpha^{\mathrm{HL}}$
- The correlations between $\lambda_\alpha^{\mathrm{PL}}$ and $\lambda_\alpha^{\mathrm{HL}}$ are used to build TMs

There is an alternative approach of "shape functions" by Korchemsky and Sterman arXiv:hep-ph/9902341

ATLAS: impact of non-perturbative corrections

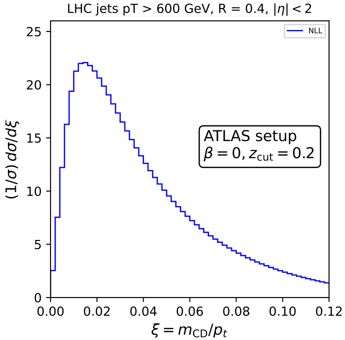

- Transfer matrix can be extracted from MC
- One needs to "put event generation on pause" when parton shower reach non-perturbative scale and calculate $\lambda_\alpha^{\mathrm{PL}}$
- After that one "resume" event generation and calculate $\lambda_\alpha^{\mathrm{HL}}$
- The correlations between $\lambda_\alpha^{\mathrm{PL}}$ and $\lambda_\alpha^{\mathrm{HL}}$ are used to build TMs

There is an alternative approach of "shape functions" by Korchemsky and Sterman arXiv:hep-ph/9902341

ATLAS: impact of non-perturbative corrections

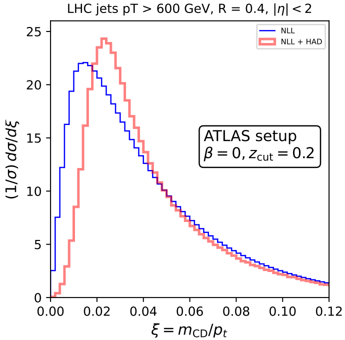

- Transfer matrix can be extracted from MC
- One needs to "put event generation on pause" when parton shower reach non-perturbative scale and calculate $\lambda_\alpha^{\mathrm{PL}}$
- After that one "resume" event generation and calculate $\lambda_\alpha^{\mathrm{HL}}$
- The correlations between $\lambda_\alpha^{\mathrm{PL}}$ and $\lambda_\alpha^{\mathrm{HL}}$ are used to build TMs

There is an alternative approach of "shape functions" by Korchemsky and Sterman arXiv:hep-ph/9902341

ATLAS: impact of non-perturbative corrections

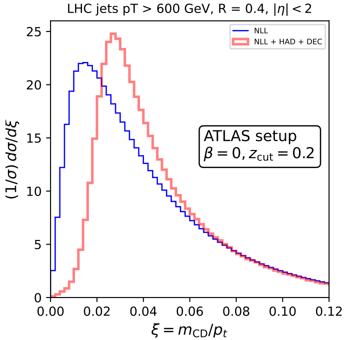

- Transfer matrix can be extracted from MC
- One needs to "put event generation on pause" when parton shower reach non-perturbative scale and calculate $\lambda_\alpha^{\rm PL}$
- After that one "resume" event generation and calculate $\lambda_\alpha^{\rm HL}$
- The correlations between $\lambda_\alpha^{\rm PL}$ and $\lambda_\alpha^{\rm HL}$ are used to build TMs

There is an alternative approach of "shape functions" by Korchemsky and Sterman arXiv:hep-ph/9902341

ATLAS: impact of non-perturbative corrections

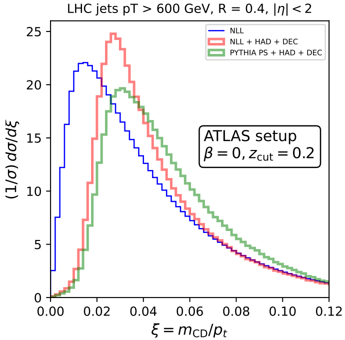

- Transfer matrix can be extracted from MC
- One needs to "put event generation on pause" when parton shower reach non-perturbative scale and calculate $\lambda_\alpha^{\rm PL}$
- After that one "resume" event generation and calculate $\lambda_\alpha^{\rm HL}$
- The correlations between $\lambda_\alpha^{\rm PL}$ and $\lambda_\alpha^{\rm HL}$ are used to build TMs

There is an alternative approach of "shape functions" by Korchemsky and Sterman arXiv:hep-ph/9902341

ATLAS: impact of non-perturbative corrections

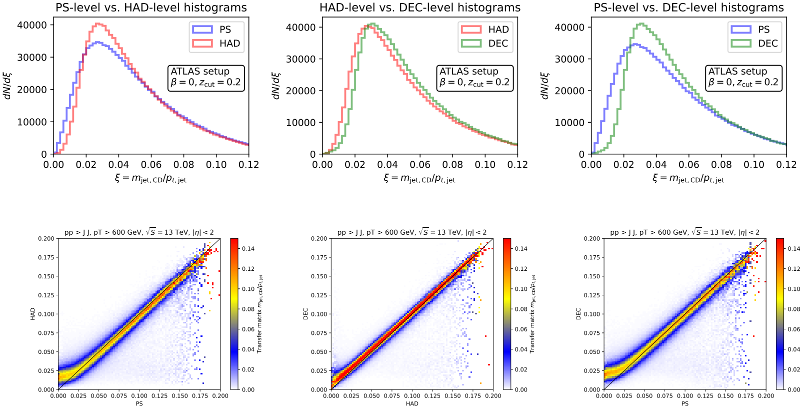

Non-perturbative corrections usually shift distributions towards larger observable values. Here we consider parton-to-hadron transition and hadronic decays separately.

STAR: impact of non-perturbative corrections

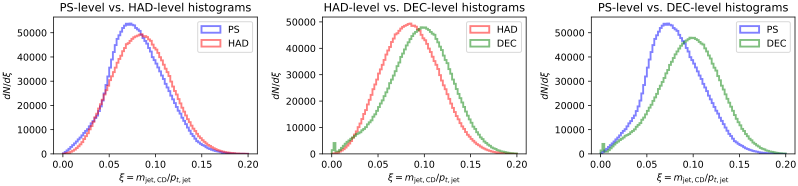

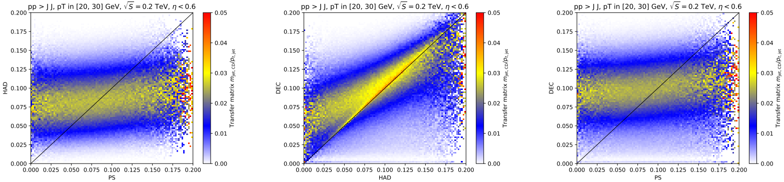

Non-perturbative corrections usually shift distributions towards larger observable values. Here we consider parton-to-hadron transition and hadronic decays separately.

Summary:

- We obtained NLL accuracy level predictions for collinear drop jet mass.
- The non-perturbative corrections and decays are incorporated via transfer matrices extracted from Pythia.
- Impact from hadron decays is large and screens hadronization.
- At LHC (high p_t jets) hadronization acts in agreement with Korchemsky and Sterman framework, whereas at RHIC (low p_t jets) there is no “shift” of the distribution.
- Transfer matrices at RHIC demonstrate universal behavior of Pythia hadronization model (different partonic configurations are hadronized in approximately the same way)
- The NLL calculations require some improvements at low observable value (Landau pole treatment) .
- Better understanding of hadronization for RHIC jets is needed.

SCET NLL results were obtained by Chien and Stewart in arXiv:1907.11107

Thank you!

Backup slides

CollinearDrop: LHC setup

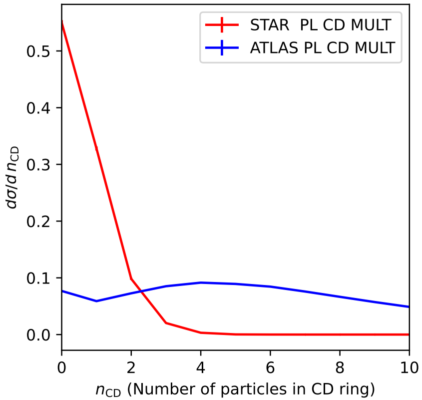

- ATLAS setup: $\sqrt{S} = 13$ TeV, $p_t > 600$, $|\eta| < 2$.
- RHIC setup: $\sqrt{S} = 0.2$ TeV, $p_t \in [20, 30]$, $|\eta| < 0.6$.
- Number of particles inside the CollinearDrop ring at RHIC is much smaller comparing to the LHC.
- Hadronization of a few ($\sim$ 1 - 3) particles will differ from hadronization of a larger set ($\sim$ 4 - 15) particles.

Theory vs. CMS data

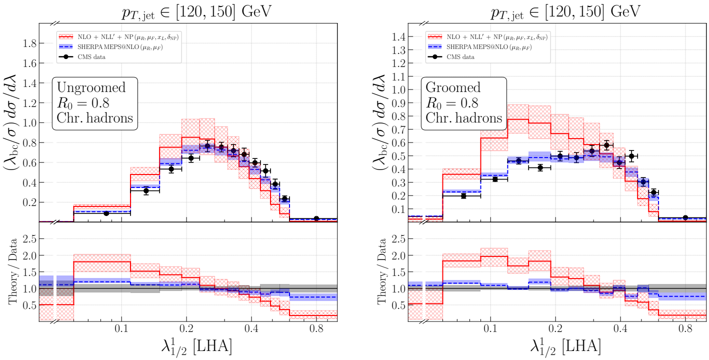

Comparison against recent CMS data for the LHA angularity, $p_{T,\mathrm{jet}} \in [120, 150]$ GeV.

Theory: 2112.09545, 2104.06920 (S. Caletti, OF, S. Marzani, D. Reichelt, S. Schumann, G. Soyez, V. Theeuwes); CMS: 2109.03340

Theory (including TM) vs. CMS data

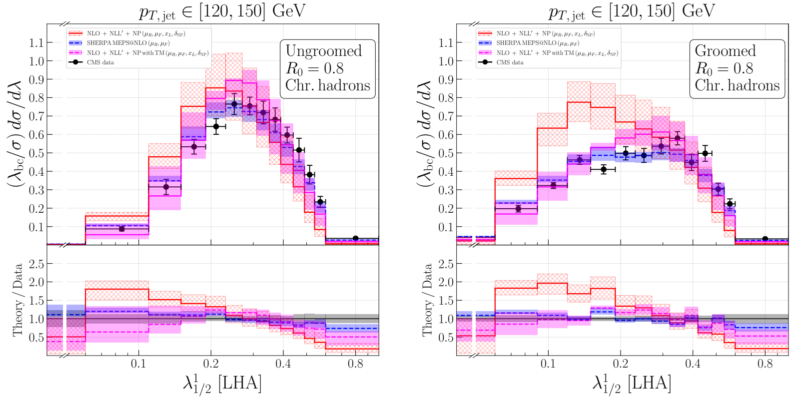

Comparison against recent CMS data for the Jet Thrust angularity, $p_{T,\text{jet}} \in [120, 150]$ GeV. Magenta band correspond to transfer matrix approach.

Theory: 2112.09545, 2104.06920 (in collaboration with S. Caletti, S. Marzani, D. Reichelt, S. Schumann, G. Soyez, V. Theeuwes); CMS: 2109.03340

Migration between different p_T-bins; credit S. Schumann

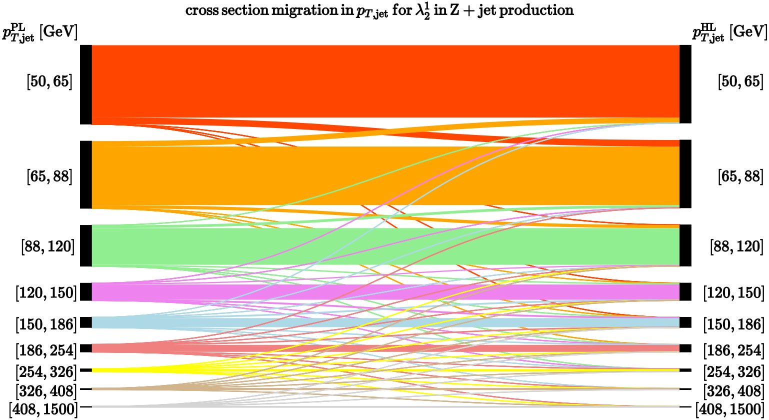

Hadronization can cause migration between different p_T-bins.

Parton to hadron level transition; credit G. Soyez

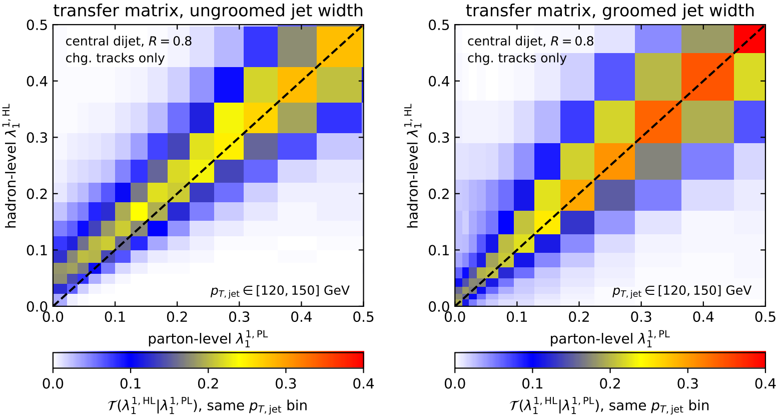

Transfer matrix $\mathcal{T}(\lambda_1^{1,\mathrm{HL}}|\lambda_1^{1,\mathrm{PL}})$ for the jet-width angularity for central dijet events with $R = 0.8$ and $p_{T,\mathrm{jet}} \in [120, 150]$ GeV.

Parton to hadron level transition; credit G. Soyez

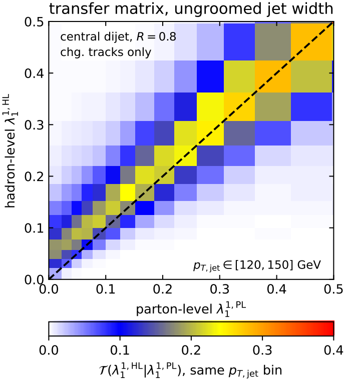

- Transfer matrix can be extracted from MC
- One needs to "put event generation on pause" when parton shower reach non-perturbative scale and calculate $\lambda_\alpha^{\mathrm{PL}}$
- After that one "resume" event generation and calculate $\lambda_\alpha^{\mathrm{HL}}$
- The correlations between $\lambda_\alpha^{\mathrm{PL}}$ and $\lambda_\alpha^{\mathrm{HL}}$ are used to build TMs

Comparison against CMS data, 2112.09545

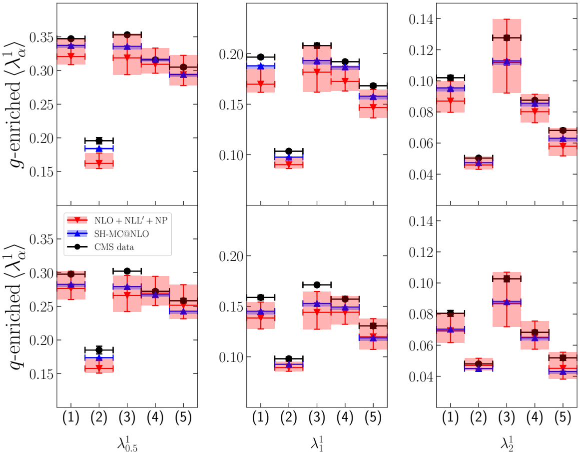

configuration	type of jet	$p_{T,\text{jet}}$ [GeV]	g-enriched	q-enriched
(1)	ungroomed $R = 0.4$	[120,150]	dijet central	Z+jet
(2)	ungroomed $R = 0.4$	[1000,4000]	dijet central	dijet forward
(3)	ungroomed $R = 0.8$	[120,150]	dijet central	Z+jet
(4)	ungroomed $R = 0.4$ (tracks only)	[120,150]	dijet central	Z+jet
(5)	SoftDrop ($\beta = 0$, $z_{\text{cut}} = 0.1$) $R = 0.4$	[120,150]	dijet central	Z+jet

RHIC and upgraded PHENIX experiment

- The PHENIX detector was upgraded to sPHENIX
- New detector has better rapidity coverage $|\eta| < 0.7$
- Can be used to study jet substructure at $\sqrt{S} = 200$ GeV

Areal view at the RHIC facility.

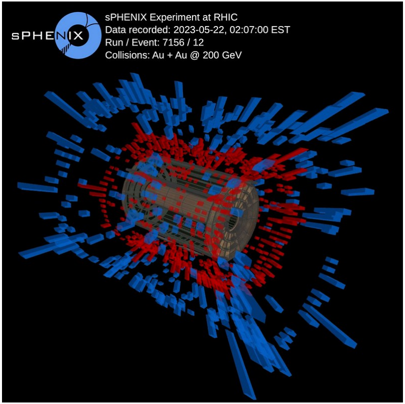

sPHENIX data taking

Image credits: BNL

Jet substructure at RHIC, 2404.04168

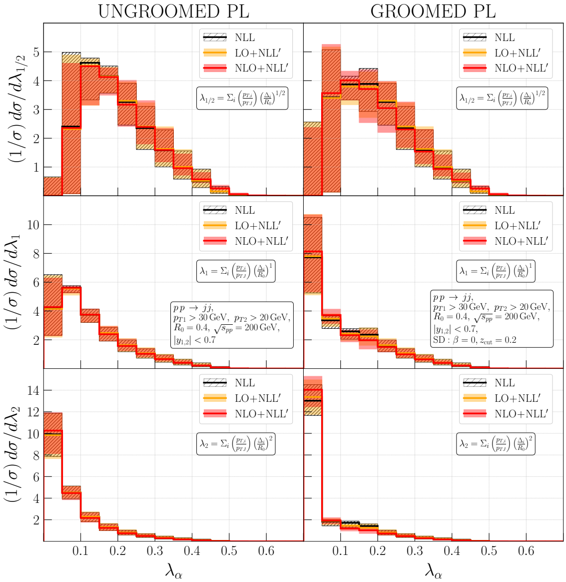

Parton-level results for LHA, Jet Width and Jet Thurst

Parton-level jet substructure at RHIC, 2404.04168

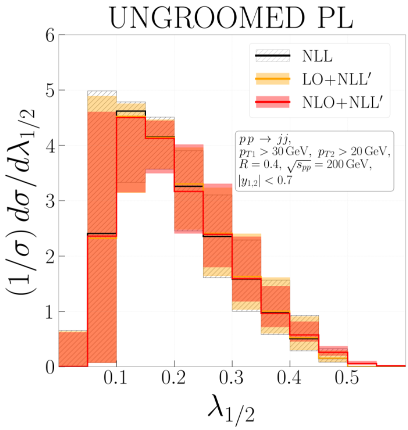

- Our results for jet angularities are at highest available accuracy NLO+NLL′ level
- Result are available for LHA, Jet Width and Jet Thrust (for ungroomed and groomed jets)
- The increase in accuracy of calculation reduces the size of uncertainty bands
- Further increase in accuracy may be necessary

Hadron-level jet substructure at RHIC, 2404.04168

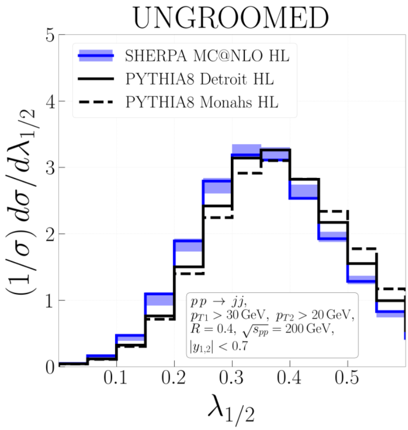

- Our results for jet angularities are at highest available accuracy NLO+NLL′ level
- Result are available for LHA, Jet Width and Jet Thrust (for ungroomed and groomed jets)
- The increase in accuracy of calculation reduces the size of uncertainty bands
- Further increase in accuracy may be necessary

Impact of non-perturbative corrections

- Unlike the LHC at RHIC non-perturbative corrections are dominant
- The bin-migration caused by hadronization shift the peak position
  - Detroit and Monash Pythia tunes give significantly different predictions

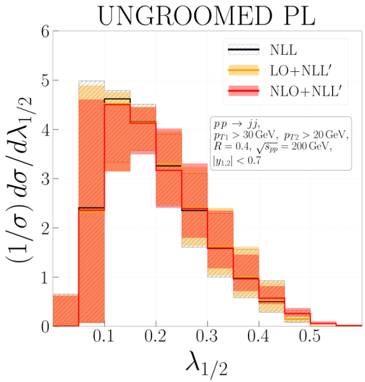

Parton-level predictions.

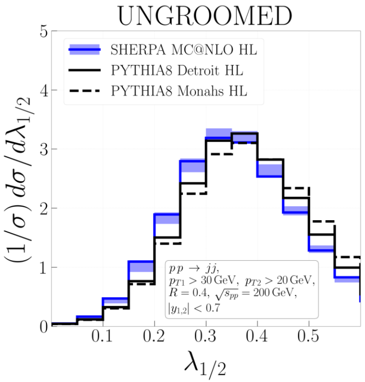

Hadron-level predictions.

Pythia tunes and MPI contribution

- Much lower collision energy at RHIC leads to suppression of MPI
  - The Detroit Pythia tune almost eliminates MPI contribution
- Jet substructure at RHIC is mostly affected by hadronization

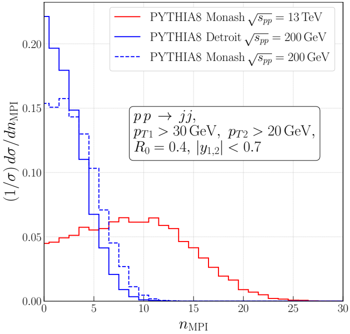

MPI multiplicity at RHIC and LHC.

TABLE I. PYTHIA 8 settings and tuning parameters.

Setting	Default	New
PDF:pSet	13	17
MultipartonInteractions:ecmRef	7 TeV	200 GeV
MultipartonInteractions:bprofile	3	2
Tuning Parameter	Default	Range
MultipartonInteractions:pT0Ref	2.28 GeV	0.5-2.5 GeV
MultipartonInteractions:ecmPow	0.215	0.0-0.25
MultipartonInteractions:coreRadius	0.4	0.1-1.0
MultipartonInteractions:coreFraction	0.5	0.0-1.0
ColourReconnection:range	1.8	1.0-9.0

Detroit Pythia tune 2110.09447.

Jet substructure in AA collisions

- We expect a new state of matter to born in AA collisions
- Particles produced via hard QCD interaction and parton shower can interact with the QGP scattering centers
- Particles produced via hard QCD interaction and parton shower can interact with the QGP scattering centers
- Thermalization of QGP creates a huge soft background

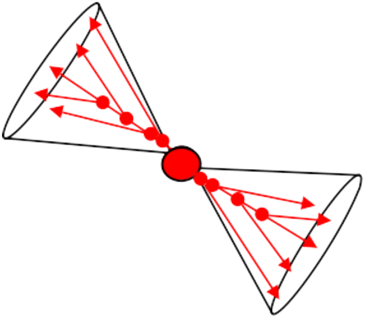

Jet quenching.

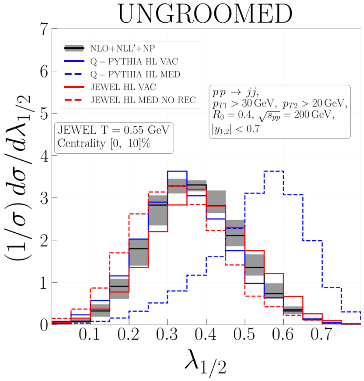

Jet substructure in AA collisions.

Jet substructure in AA collisions

- We expect a new state of matter to born in AA collisions
- Particles produced via hard QCD interaction and parton shower can interact with the QGP scattering centers
- Particles produced via hard QCD interaction and parton shower can interact with the QGP scattering centers
- Thermalization of QGP creates a huge soft background

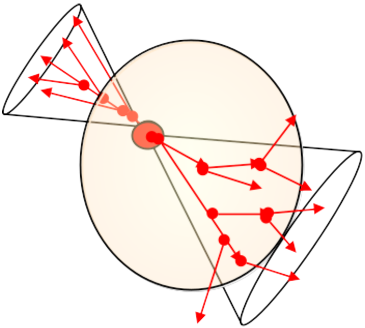

Jet quenching.

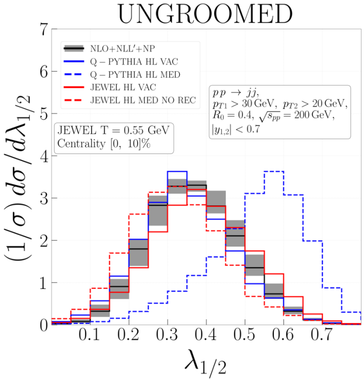

Jet substructure in AA collisions.

Jet substructure in AA collisions

- We expect a new state of matter to born in AA collisions
- Particles produced via hard QCD interaction and parton shower can interact with the QGP scattering centers
- Particles produced via hard QCD interaction and parton shower can interact with the QGP scattering centers
- Thermalization of QGP creates a huge soft background

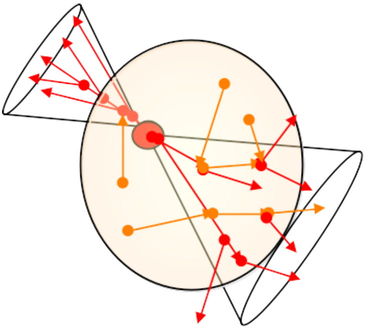

Jet quenching.

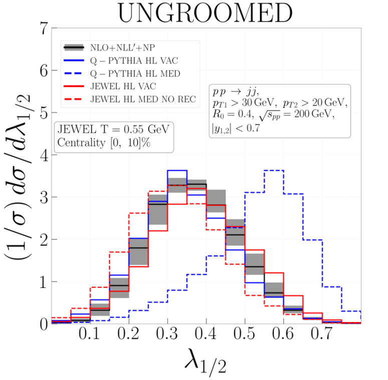

Jet substructure in AA collisions.

Jet substructure in AA collisions

- We expect a new state of matter to born in AA collisions
- Particles produced via hard QCD interaction and parton shower can interact with the QGP scattering centers
- Particles produced via hard QCD interaction and parton shower can interact with the QGP scattering centers
- Thermalization of QGP creates a huge soft background

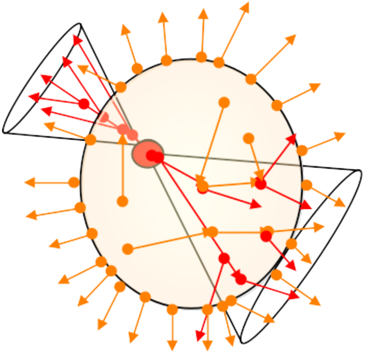

Jet quenching.

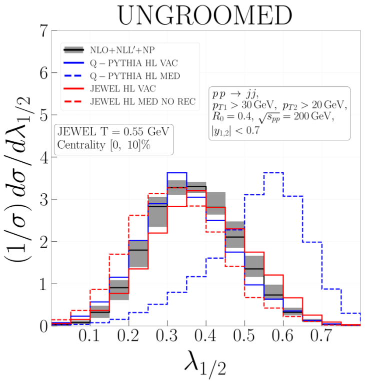

Jet substructure in AA collisions.

Jet substructure in AA collisions

- We expect a new state of matter to born in AA collisions
- Particles produced via hard QCD interaction and parton shower can interact with the QGP scattering centers
- Particles produced via hard QCD interaction and parton shower can interact with the QGP scattering centers
- Thermalization of QGP creates a huge soft background

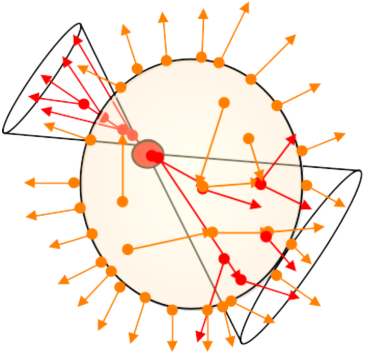

Jet quenching.

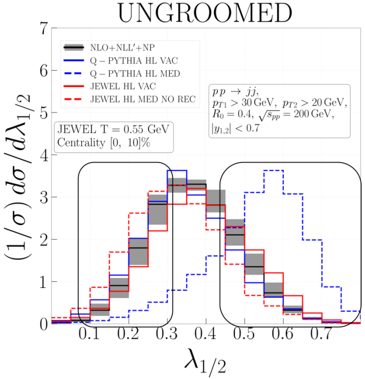

Jet substructure in AA collisions.

Discrepancy between different quenching models

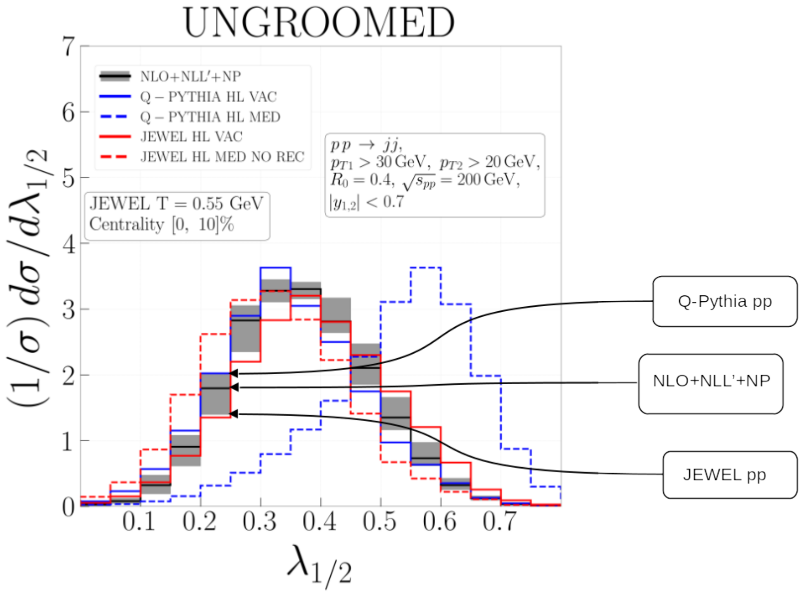

Discrepancy between different quenching models